Optimization of length and thickness of smart transduction layers on beam structures for control and M/NEMS applications

Olivier Thomas, Bernard Legrand, Cécile Fuinel

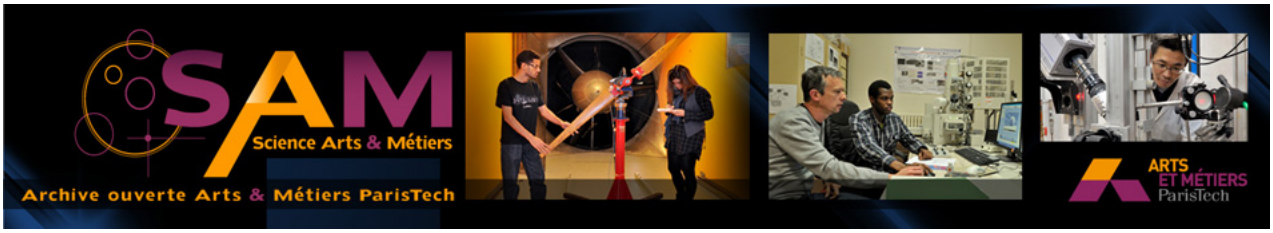

OPTIMIZATION OF LENGTH AND THICKNESS OF SMART TRANSDUCTION LAYERS ON BEAM STRUCTURES FOR CONTROL AND M/NEMS APPLICATIONS

Olivier Thomas*
Arts et Métiers ParisTech
LSIS UMR CNRS 7296
8 bd. Louis XIV 59046 Lille, France
olivier.thomas@ensam.eu

Bernard Legrand, Cécile Fuinel
LAAS-CNRS,
7 avenue du Colonel Roche, F-31077, Toulouse, France
bernard.legrand@laas.fr
cecile.fuinel@laas.fr

ABSTRACT

This work addresses the optimization of the geometry of smart sensors and actuators on cantilever beams. Three transduction principles are studied and compared in term of efficiency: piezoelectric, electrostatic and dielectric. For the piezoelectric transduction, an active layer of a shorter length than the one of the beam is added on its surfaces. For the electrostatic transduction, the beam is made of a conducting material and it is faced with a fixed electrode at a distance called the gap. This architecture is widely used for M/NEMS (Micro/Nano ElectroMechanical Systems). The last transduction principle, new and promising, is based on the use of dielectric layers on the beam surface. In this case, the excitation is based on electrostatic forces between the charged electrodes, causing transverse deformation of the dielectric film and bending of the multilayer structure; the detection of the vibration is capacitive, based on the fluctuation of the capacitance due to the deformation of the dielectric film. This work presents the optimization of the length and the thickness of the piezoelectric/dielectric layers and, for the electrostatic case, the optimization of the length and the gap of the electrostatic cavity. The study is based on an analytic model for a laminated beam and closed-form formula of the optimization parameters (coupling factor, driving efficiency, sensing efficiency) are obtained. The application of those three transduction principles mainly focus on resonating M/NEMS sensors, whereas the case of piezoelectric transduction is also useful for vibration control of macro-structures, especially with passive shunt techniques. General results on the comparison of the transduction efficiency, as a function of the device size and of the material properties, are also derived.

INTRODUCTION

The coupling of a mechanical structure elasticity to an electronic circuit is often use in modern applications. For macro-structures (of human size), piezoelectric materials are often used for their ability to convert the mechanical energy of the structure they are bonded on into electrical and conversely. Applications are sensors, actuators or, in the case of vibrations, control or energy harvesting [1, 2]. In the case of micro or nano structures, the traditional transduction principle is electrostatics, for which the mechanical structure is made of a conducting material and it is faced with a fixed electrode at a distance called the gap [3]. For actuation, a voltage is imposed between the structure and the electrode, which creates an electrostatic pressure on the structure. For detection, one monitors the electric charge variations in the electrode, that are linked to the change of the electric capacitance due to the gap variations when the structure bends. Piezoelectric transduction is also often used for micro/nano structures [4, 5]. In this work, a promising new transduction principle, introduced in [6] and denoted by "dielectric transduction", is also studied. It is based on the use of dielectric layers on the beam surface. In this case, the excitation is based on electrostatic forces between the charged electrodes, causing transverse deformation of

*Address all correspondence to this author.

the dielectric film and bending of the multilayer structure due to Poisson's effect; the detection of the vibration is capacitive, based on the fluctuation of the capacitance due to the transverse deformation of the dielectric film.

The goals of the present work are following. First, a model for the dielectric transduction principle is proposed. It is shown that in the case of thin dielectric layers, it is possible to formulate the dielectric transduction on the form of a classical piezoelectric constitutive law, with a particular value for the transduction constant d_{31}. Then, the three transduction principles (piezoelectric, dielectric and electrostatic) are compared in term of efficiency. Finally, the effect of the geometry of the transduction layers (length, thickness and position on the structure for piezoelectric and dielectric; length and position of the electrode for electrostatic) on the transduction efficiency are studied, in order to optimize the electromechanical structure. Two efficiency indicator families are considered: (i) the modal electromechanical coupling factor (MEMCF), useful for passive control applications such as piezoelectric shunts (ii) several transduction indicators for resonant Micro/Nano Electro Mecanical Systems (M/NEMS). A cantilever beam is considered as a test structure. One issue addressed in particular is the mechanical effect (mass and stiffness addition) of the piezoelectric/dielectric layer on the optimization process, thanks to the multilayer modelling of the beam: can we neglect it ? In optimization of passive control with piezoelectric shunts, some studies prove that it cannot be neglected [7, 8]. Is it the same for optimization of resonant M/NEMS sensors ?

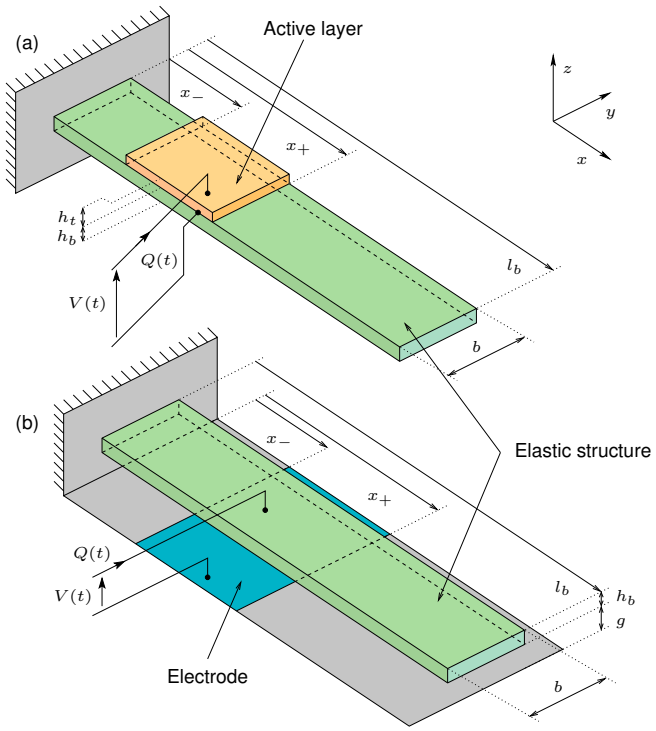

Figure 1. ELASTIC BEAMS WITH ELECTROMECHANICAL TRANSDUCTION (a) BEAM WITH AN ACTIVE LAYER; (b) BEAM WITH ELECTROSTATIC TRANSDUCTION

Modelling of the electromechanical structures

The electromechanical structures under study are sketched on Fig. 1. For the piezoelectric and dielectric actuation, one active layer is considered, so that the structure has the form of a laminated beam, whose cross section geometry depends on the axial coordinate x. For the electrostatics transduction, the beam's cross-section geometry is assumed uniform. In the two cases, the beam kinematics is based on the classical Euler-Bernoulli assumptions: each beam cross section remain plane and normal. The model exposed in [7, 9] is used. It is based on the classical continuum mechanics theory, that is assumed to apply to the small scale devices considered in this work (for NEMS with no dimension under 100 nm [10]). The displacement field writes:

$$\begin{cases} u_x(x,y,z,t) = u(x,t) - z\, w_{,x}(x,t), & (1) \\ u_z(x,y,z,t) = w(x,t), & (2) \end{cases}$$

where t is the time, u_x and u_z are the axial and transverse displacement of the point of coordinates (x, y, z); u is the beam center line axial displacement and w its transverse displacement; $(\cdot)_{,x}$ denotes a partial derivative with respect to x. The displacement u_y in the y-axis direction is not considered in this work. The only non-zero strain tensor component is:

$$\varepsilon_x = u_{x,x} = u_{,x} - z w_{,xx}. \qquad (3)$$

The electric state of the electromechanical structures is defined by the electric field and the electric displacement under the electrostatic approximation [11]. The electric field is assumed to be transverse and uniform, so that the potential difference V between the electrodes of an active layer of thickness h_t, or between the elastic structure and the lower electrode (separated by a gap g, in the case of the electrostatic transduction), is:

$$V(t) = -E_z(t) h_t, \qquad \text{or} \qquad V(t) = -E_z(t) g, \qquad (4)$$

where E_z is the transverse component of the electric field.

Piezoelectric transduction

For a piezoelectric active layer, the following linear constitutive law is considered:

$$\begin{cases} \sigma_x = Y_p\,\varepsilon_x - e_{31}\,E_z & \text{(5a)} \\ D_z = e_{31}\,\varepsilon_x + \epsilon_p\,E_z & \text{(5b)} \end{cases}$$

where σ_x and D_z are the axial stress and the transverse electric displacement, Y_p is the piezoelectric material Young's modulus in the (x, y) plane at constant electric field, e_{31} is the modified piezoelectric constant and ϵ_p is the modified dielectric permittivity at constant strain, when beam assumptions are formulated ($\sigma_y = \sigma_z = 0$) [9]. In particular, $e_{31} = Y_p\,d_{31}$ where d_{31} is the usual 3D piezoelectric constant.

For a thin piezoelectric layer ($h_t \ll l_b$ with l_b the length of the beam), the electric field E_z is assumed normal to the electrodes and uniform (the fringe effects are neglected as well as a possible linear dependence as a function of z [9]). Integrating the above constitutive law across the area of the beam's cross section and across the electrodes area (situated between $x = x_-$ and $x = x_+$) lead to the following relations between the generalized quantities: the bending moment M and the electric charge Q contained in the upper electrode [7]:

$$\begin{cases} M = -Dw_{,xx} + \Theta U(x)V, & \text{(6a)} \\ Q = \Theta\big[w_{,x}\big]_{x_-}^{x_+} + C_pV, & \text{(6b)} \end{cases}$$

where

$$U(x) = \varsigma(x - x_-) - \varsigma(x - x_+), \tag{7}$$

where $\varsigma(x)$ is the Heavyside step function ($\varsigma(x) = 0\ \forall x < 0$; $\varsigma(x) = 1\ \forall x \geq 0$). In the above equations, $D(x)$ is the beam's bending stiffness (in short circuit $V = 0$), Θ is the piezoelectric coupling coefficient and C_p is the blocked capacitance of the active layer. Those three parameters depend on the geometrical and material characteristic of laminated structure of the cross section.

The above equations assume no axial/bending coupling, a case valid for a symmetric lamination in the transverse direction. In the present case, the lamination between x_- and x_+ is asymmetric (see Fig. 1(a)). However, with clamped/free boundary conditions for which the axial force is zero, the axial motion is slaved to the bending motion and the above equations are still valid with modified values of D, Θ and C_p. They write [7]:

$$\Theta = \frac{be_{31}(h_b + h_t)}{\underbrace{2(1+\kappa)}}, \qquad C_p = \frac{\epsilon_p b l_t}{h_t}\underbrace{\left(1 + \frac{k_{31}^2\kappa}{1+\kappa}\right)} \tag{8}$$

where $\kappa = Y_p h_t/(Y_b h_b)$ and $k_{31} = e_{31}/\sqrt{\epsilon_p Y_p}$. The axial/bending coupling is responsible of the two additional underlined terms.

The beam's equation of motion is [7]:

$$m\ddot{w} + [Dw_{,xx}]_{,xx} - \Theta\Delta(x)V = p, \tag{9}$$

where $m(x)$ is the beam's mass per unit length, $p(x,t)$ is the external transverse forces per unit length and $\Delta(x) = [\delta(x - x_-)_\delta(x - x_+)]_{,x}$ with $\delta(x)$ the Dirac function.

Dielectric layer transduction

For a dielectric layer, we formulate the same assumptions than the one used for a piezoelectric layer [9]: the dielectric layer is thin and covered by conductive electrodes (of negligible thickness), and the electric field E_z is assumed uniform. In this case, when the dielectric layer is subjected to the electric field E_z, electric charges of opposite sign appear in the electrodes, which create an attractive force between the electrodes. The dielectric layer is thus submitted to a compressing force per unit area f [12, p. 103], that creates a non zero z component of the stress in the dielectric layer:

$$\sigma_z = f = -\frac{\epsilon_d}{2}E_z^2, \tag{10}$$

where ϵ_d is the permittivity of the dielectric material. Furthermore, the dielectric layer is considered linear elastic, so that its 3D constitutive law writes:

$$\begin{cases} \varepsilon_x = \dfrac{1}{Y_d}\left[\sigma_x - \nu\left(\sigma_y + \sigma_z\right)\right], & \text{(11a)} \\ \varepsilon_y = \dfrac{1}{Y_d}\left[\sigma_y - \nu\left(\sigma_x + \sigma_z\right)\right], & \text{(11b)} \\ \varepsilon_z = \dfrac{1}{Y_d}\left[\sigma_z - \nu\left(\sigma_x + \sigma_y\right)\right], & \text{(11c)} \\ D_z = \epsilon_d E_z & \text{(11d)} \end{cases}$$

where Y_d and ν are the Young's modulus and the Poisson's ratio of the dielectric material. In the same manner than for a piezoelectric layer, since the considered structures are beams, we assume that the stress in the y-direction vanishes: $\sigma_y = 0$.

The converse electromechanical coupling in the dielectric layers is the result of its change of thickness due to $f = \sigma_z$, that changes its length due to the Poisson's effect. We then obtain, with Eq. (11a), $\sigma_y = 0$ and Eq. (10):

$$\sigma_x = Y_d\,\varepsilon_x - \frac{\nu\epsilon_d}{2}E_z^2 \tag{12}$$

The direct electromechanical coupling is also the result of the change of thickness of the dielectric layer, that changes its electrical capacitance. The current thickness of the dielectric layer is $h_d(1+\varepsilon_z)$, so that the electric field in the layer is related to the potential difference between the electrodes with:

$$E_z = -\frac{V}{h_d(1+\varepsilon_z)} \simeq -\frac{V}{h_d}(1-\varepsilon_z), \tag{13}$$

where ε_z is assumed small. Using Eq. (11c) and (12) gives:

$$\varepsilon_z = -\nu\varepsilon_x - \frac{(1-\nu^2)\epsilon_d}{2Y_d}E_z^2. \tag{14}$$

The local electromechanical coupling laws for the dielectric layer are then:

$$\begin{cases} \sigma_x = Y_d\,\varepsilon_x - \dfrac{\nu\epsilon_d}{2}\left(\dfrac{V}{h_d}\right)^2, & \text{(15a)} \\ D_z = -\dfrac{\nu\epsilon_d V}{h_d}\,\varepsilon_x - \epsilon_d\dfrac{V}{h_d}. & \text{(15b)} \end{cases}$$

They are obtained by (i) introducing (13) in (12) and (ii) by introducing (14) in (13) and the result in (11d) and (iii) neglecting any higher order term than the quadratic ones in (V, ε_x).

In practice, a linear electromechanical coupling can be obtained by superimposing a DC voltage V_{dc} to the fluctuating voltage: $V(t) = V_{\text{dc}} + \tilde{V}(t)$. In this case, Eqs. (15a,b) becomes:

$$\begin{cases} \tilde{\sigma}_x = Y_d\,\varepsilon_x - \dfrac{\nu\epsilon_d V_{\text{dc}}}{h_d}\dfrac{\tilde{V}}{h_d}, & \text{(16a)} \\ \tilde{D}_z = -\dfrac{\nu\epsilon_d V_{\text{dc}}}{h_d}\,\varepsilon_x - \epsilon_d\dfrac{\tilde{V}}{h_d}. & \text{(16b)} \end{cases}$$

where $\tilde{\sigma}_x = \sigma_x + \nu\epsilon_d V_{\text{dc}}^2/2h_d^2$ and $\tilde{D}_z = D_z + \epsilon_d V_{\text{dc}}/h_d$ are the fluctuating axial stress and electric displacement. Note that the quadratic nonlinear terms in $(\tilde{V}, \varepsilon_x)$ have been neglected. Eqs. (16a,b) are formally equivalent to the piezoelectric constitutive law (5a,b) with equivalent piezoelectric coefficients[1]

$$e_{31} = \frac{\nu\epsilon_d V_{\text{dc}}}{h_d} \quad \text{or} \quad d_{31} = \frac{\nu\epsilon_d V_{\text{dc}}}{h_d Y_d} \tag{17}$$

As a consequence, *any dielectric thin layer is analogous to a piezoelectric layer*, so that any structure including dielectric layers can be modelled in the same way as if the dielectric layers were piezoelectric. In particular, the generalized constitutive laws (6a,b) and the equation of motion (9) are still valid for the dielectric layers transduction.

[1] When comparing Eqs. (16a,b) to (5a,b) to identify e_{31}, and especially its sign, one has to recall that $\tilde{V}/h_d$ in (16a,b) is the *opposite* of an electric field

Electrostatic transduction

For the electrostatic transduction, the beam is built in a conductive material and behaves like an electrode. When a potential difference $V(t)$ is applied between the beam and the bottom electrode (Fig. 1(b)), an electrostatic attractive force appears. We assume, in the same manner than for the active layers, that the gap between the beam and the bottom electrode is thin ($g \ll l_b$), so that the electric field is normal to the electrodes and uniform. The beam is thus submitted to a force analogous to the one of Eq. (10), applied only on the area faced by the bottom electrode, between $x = x_-$ and $x = x_+$. By considering that $V(t) = V_{dc} + \tilde{V}$, the equation of motion is:

$$m\ddot{w} + Dw_{,xxxx} - \Theta_e U(x)\tilde{V} = p, \quad \Theta_e = -\frac{b\epsilon_0 V_{\text{dc}}}{g^2}, \tag{18}$$

where ϵ_0 is the gap (vacuum) permittivity, b is the beam's width and $U(x)$ is defined by Eq. (7).

For the sensing effect, the charge in the electrodes is obtained in the same way than for the dielectric actuation. The electric displacement and field in the gap are:

$$D_z = \epsilon_0 E_z, \quad E_z = \frac{V}{g-w} \simeq \frac{V}{g}\left(1+\frac{w}{g}\right). \tag{19}$$

Then, integrating D_z over the area faced by the electrode gives:

$$Q = \Theta_e \int_{x_-}^{x^+} w\ \mathrm{d}x + C_e V, \qquad C_e = \frac{\epsilon_0 b l_t}{g}, \tag{20}$$

where C_e is the capacitance of the cavity between the bottom electrode and the beam, with $l_t = x_+ - x_-$ the electrode length.

Modal expansion

We discretize the beam's transverse displacement field with the following modal expansion:

$$w(x,t) = \sum_{i=1}^{N} \Phi_i(x) q_i(t) \tag{21}$$

where $q_i(t)$ is the i-th modal coordinate and (Φ_i, ω_i), $i = 1 \ldots N$ are the first N short circuit eigenmodes of the beam, defined by the following generalized eigenvalue problem:

$$[D\Phi_{i,xx}]_{,xx} - \omega_i \Phi_i = 0. \tag{22}$$

Then, substituting Eq. (21) into Eqs. (9,6b) and (18,20), multiplying the result by Φ_j, integrating the equation of motion over the length of the beam and using the orthogonality properties of the (Φ_i, ω_i), leads to:

$$\begin{cases} \ddot{q}_i + 2\xi_i\omega_i\dot{q}_i + \omega_i^2 q_i - \chi_i/M_i\tilde{V} = 0, \quad \forall i = 1, \dots N & \text{(23a)} \\ Q = \sum_{i=1}^{N} \chi_i q_i + C\tilde{V} & \text{(23b)} \end{cases}$$

where the modal electromecanical coupling coefficient χ_i and capacitance C are:

$$\text{piezo./dielectric transduction :} \quad \chi_i = \Theta \left[\Phi_{i,x}\right]_{x_-}^{x_+} \quad \text{(24a)}$$

$$C = C_p \quad \text{(24b)}$$

$$\text{electrostatic transduction:} \quad \chi_i = \Theta_e \int_{x_-}^{x_+} \Phi_i \, \mathrm{d}x \quad \text{(24c)}$$

$$C = C_e \quad \text{(24d)}$$

and the i-th. modal mass is:

$$M_i = \int_0^{l_b} m(x)\Phi_i^2(x) \, \mathrm{d}x, \qquad \text{[kg]} \qquad (25)$$

OPTIMIZATION CRITERIA

The efficiency of the electromechanical transduction depends on the purpose of the device and several optimization criteria may be defined.

Modal coupling coefficient

The *modal coupling coefficient* is the parameter χ_i that appears in Eqs. (23). Its physical meaning is that it characterize either the modal force that is created per unit of input voltage or the electric charge that is created per unit modal displacement. It can be expressed in [N/V] or [C/m]. It depends on the scaling of the deformed shapes Φ_i.

Resonant displacement criterion

The electromechanical transduction may be used as an actuation mean to create a resonant motion of the device. We consider the tip displacement of a cantilever beam submitted to a voltage $\tilde{V} = V_0 \cos\Omega t$ at resonance ($\Omega \simeq \omega_i$). Using Eqs. (21) and (23a) reduced to a single mode, one obtains the tip displacement amplitude w_0 at the i-th resonance. It enable to define the following *actuation efficiency* criterion:

$$\eta_{\text{act}} = \frac{w_0}{V_0} = \frac{|\chi_i\Phi_i(l_b)|}{2\xi\omega_i^2 M_i} = \frac{|\chi_i\Phi_i(l_b)|}{2\xi K_i} \qquad \text{[m/V]} \qquad (26)$$

where $K_i = \omega_i^2 M_i$ is the modal stiffness of the i-th. mode.

Motional capacitance / conductance criteria

If the device is used as a mass sensor (see [4] and reference therein), one is interested in maximizing the electric charge quantity (or the electric current intensity) that is generated at the terminals of the active layer when this active layer drives the device at a given resonance. In this case, the motional part of the generated electric charge[2] is (Eq. 23b) $Q_{\text{mot}} = \chi_i q_i$ and the current intensity amplitude is $I_0 = \omega_i Q_0$ (where $Q_{\text{mot}} = Q_0 \cos(\Omega t + \varphi)$) since the device is run at $\Omega \simeq \omega_i$. This enables to define the two following optimization criteria: *the motional capacitance*:

$$C_{\text{mot}} = \frac{Q_0}{V_0} = \frac{\chi_i^2}{2\xi\omega_i^2 M_i} = \frac{\chi_i^2}{2\xi K_i} \qquad \text{[C/V]}$$

and the *motional conductance*:

$$G_{\text{mot}} = \frac{I_0}{V_0} = \frac{\chi_i^2}{2\xi\omega_i M_i} = \frac{\chi_i^2}{2\xi\sqrt{K_i M_i}} \qquad \text{[A/V]}$$

Electromechanical coupling factor

The electromechanical transduction can be used for passive vibration damping, by shunting the active layer with a dedicated electrical circuit (see [13] and reference therein or [14]). Basic electrical circuits are a simple resistance, that acts as an added viscous damper, or a resistance plus an inductance, that creates a resonant circuit that can be tuned on the mechanical resonance to be damped. Other techniques enhance the performance of the two basic shunts by adding in the circuit a switch whose open and close states are synchronized to the mechanical structure oscillations. In all these cases, it can be shown (see e.g. [13, 15]) that the performance of the system in term of vibration reduction are function of only one parameter: the modal electromechanical coupling factor (MEMCF) denoted here as k_i for the i-th mode. It can be defined by a proper scaling of Eqs. (23a,b) (see [7, 9]) or more physically by the following effective coupling factor:

$$k_i = \sqrt{\frac{(\omega_i^{\text{oc}})^2 - (\omega_i^{\text{sc}})^2}{(\omega_i^{\text{sc}})^2}}$$

where $\omega_i^{\text{sc}} = \omega_i$ and ω_i^{oc} are the natural frequencies of the beam when the active layer is respectively in short-circuit ($V = 0$) or in open circuit ($Q = 0$). In our case, imposing $Q = 0$ in Eq. (23b) and substituting for $\tilde{V}$ in Eq. (23a) leads to $(\omega_i^{\text{oc}})^2 \simeq \omega_i^2 + \chi_i^2/(CM_i)$ and:

$$k_i = \frac{\chi_i}{\omega_i\sqrt{CM_i}} = \frac{\chi_i}{\sqrt{CK_i}} \qquad \text{[non dim.]} \qquad (27)$$

[2] the part of the electric charge that is generated by the motion of the structure

The above expression for ω_i^{oc} and k_i have been obtained by reducing the multi-mode model (23a,b) to only one mode ($q_j = 0$, $\forall j \neq i$).

The MEMCF is a measure of the energy that can be exchanged between the electrical circuit and the mechanical structure [16] in a given modal motion. It is also a measure of the efficiency of the active layers when they are used as both sensors and actuators at the same time.

COMPARISON OF EFFICIENCY

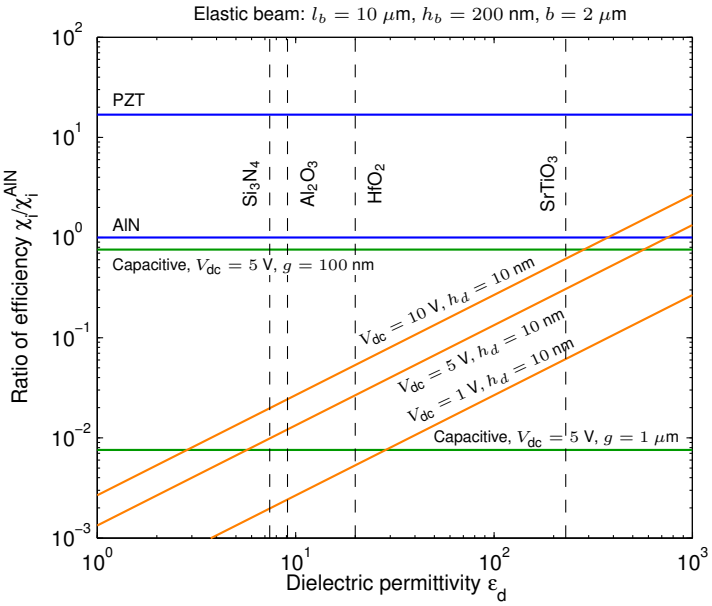

Material	e_{31} [C/m^2]	ν	ϵ_d [F/m]
PZT	14	-	-
AlN	0.83	-	-
Si_3N_4	-	0.33	$7.4\epsilon_0$
Al_2O_3	-	0.24	$9.1\epsilon_0$
HfO_2	-	0.3	$20\epsilon_0$
$SrTiO_3$	-	0.23	$230\epsilon_0$

$\epsilon_0 = 8.854$ F/m

Figure 2. COMPARISON OF EFFICIENCY (FROM EQS. (28a,b)) BETWEEN PIEZOELECTRIC (blue), DIELECTRIC (orange) AND CAPACITIVE (green) TRANSDUCTIONS.

To compare the efficiency of the three transduction principles, we consider the modal coupling coefficient χ_i (Eqs. (24a,c)) and we define the following ratios:

$$\frac{\chi_i^{\text{dielec}}}{\chi_i^{\text{piezo}}} = \frac{\nu \epsilon_d V_{\text{dc}}}{e_{31}\, h_d} \tag{28a}$$

$$\frac{\chi_i^{\text{electrostat}}}{\chi_i^{\text{piezo}}} = \frac{\epsilon_0 V_{\text{dc}} l_b^2}{e_{31}\, g^2 h_b} \frac{\displaystyle\int_{x_-}^{x_+} \Phi_i \, \mathrm{d}x}{\left[\Phi_{i,x}\right]_{x_-}^{x_+}} \tag{28b}$$

The first ratio, that compares the efficiency of the piezoelectric and dielectric layer, is simply the ratio of the e_{31} constants for the dielectric layer (Eq. (17)) and the piezoelectric layer. The second ratio, that compares the electrostatic transduction with respect to the piezoelectric one, is obtained by considering the value of Θ_e (Eq. (18)) and the one of Θ (Eq. (8)), in the case of a very thin active layer ($\kappa \simeq 0$).

To illustrate those results, the fundamental vibration mode of a nano-beam of length $l_b = 10$ μm, width $b = 2$ μm and thickness $h_b = 200$ nm is considered with an active layer / electrode that covers the whole length of the beam ($x_- = 0$, $x_+ = l_b$). The efficiency of the AlN piezoelectric material is considered as a reference. Here are some remarks.

- The standard values for e_{31} (for usual piezoelectric materials) and V_{dc} are of the order of 1 or 10, in S.I. units. As a consequence, the efficiency of the dielectric layer and the electrostatic transduction can be comparable to the one of the piezoelectric layer *only for nano-beams*, for which h_d and g are between the nanometer and the micrometer. This is because the value of g and h_d must balance the one of the permittivity ϵ_0 and ϵ_d, of the order of 10^{-11} F/m.
- The efficiency of the dielectric layer is directly proportional to its permittivity ϵ_d. Associated to a design with very thin layers (down to 10 nm, technically possible with the chosen dielectric materials), it is possible to achieve *a dielectric transduction of equivalent efficiency* to those of standard piezoelectric layer and electrostatic design, especially with $SrTiO_3$ material.

OPTIMIZATION OF THE GEOMETRY

We are interested here in choosing the geometry of the active layer that maximizes the performances of the devices. We propose to optimize the thickness h_t of the active layer (or the gap g for the electrostatic transduction), the length $l_t = x_+ - x_-$ of the active layer / electrode and their location on the beam, characterized by x_-.

Optimization with the η_{act}, C_{mot} and G_{mot} criteria

The three criteria η_{act}, C_{mot} and G_{mot} are first written as functions of the geometry parameters h_t (or g), l_t and x_-. We denote

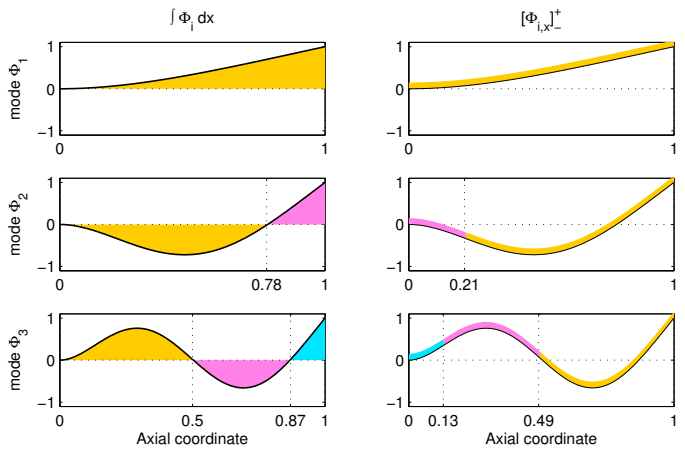

Figure 3. THE FIRST THREE MODE SHAPES OF A CANTILEVER BEAM SHOWING THE MAXIMAL VALUE OF $\int_{\bar{x}_-}^{\bar{x}_+} \Phi_i \, \mathrm{d}x$ (BY SHADED AREAS, LEFT COLUMN) AND $\left[\Phi_{i,x}\right]_{\bar{x}_-}^{\bar{x}_+}$ (BY COLORED ACTIVE LAYERS WITH OPTIMAL LOCATION AND LENGTH, RIGHT COLUMN)

by $D_b = bY_b h_b^3/12$ and $m_b = b\rho_b h_b$ the bending stiffness and mass per unit length of the beam in the part not covered by the active layer, and D_t and m_t the same quantities in the part covered by the active layer (between x_- and x_+). ρ_b is the mass density of the beam's material. It is convenient to render dimensionless (denoted with overbars) the terms that depends on Φ_i and ω_i, in the following way:

$$\bar{x} = \frac{x}{l_b}, \quad \omega_i = \frac{1}{l_b}\sqrt{\frac{D_t}{m_t}}\bar{\omega}_i \tag{29}$$

Moreover, the mode shapes are normalized so that $M_i = m_t l_b$ for all the modes.

Electrostatic actuation For the electrostatic actuation, one obtains:

$$\eta_{\text{act}} = \frac{6\,\epsilon_0 V_{\text{dc}}\, l_b^4}{\xi\, Y_b\, g^2 h_b^3} \frac{\left|\Phi_i(l_b)\ \int_{\bar{x}_-}^{\bar{x}_+} \Phi_i \, \mathrm{d}\bar{x}\right|}{\bar{\omega}_i^2} \tag{30a}$$

$$C_{\text{mot}} = \frac{6\,b\,\epsilon_0^2 V_{\text{dc}}^2\, l_b^5}{\xi\, Y_b\, g^4 h_b^3} \frac{\left[\int_{\bar{x}_-}^{\bar{x}_+} \Phi_i \, \mathrm{d}\bar{x}\right]^2}{\bar{\omega}_i^2} \tag{30b}$$

$$G_{\text{mot}} = \frac{\sqrt{3}\,b\,\epsilon_0^2 V_{\text{dc}}^2\, l_b^3}{\xi\,\sqrt{\rho_b Y_b}\, g^4 h_b^2} \frac{\left[\int_{\bar{x}_-}^{\bar{x}_+} \Phi_i \, \mathrm{d}\bar{x}\right]^2}{\bar{\omega}_i} \tag{30c}$$

In this case, since there is no active layer, the mechanics of the beam does not depend on the "active part" of the device: the deformed shapes Φ_i and the reduced frequencies $\bar{\omega}_i$ do not depend on the optimization parameters g, x_- and l_t. The optimization is then reduced to maximizing the factor $\int_{\bar{x}_-}^{\bar{x}_+} \Phi_i \, \mathrm{d}\bar{x}$. The result is displayed on Fig. 3(left column) by shaded areas. It shows that for the i-th. mode, there are i maximum solutions. However, for all modes, the optimal solution is an electrode that covers the distance between the clamped end and the location of the first node of the mode shape (since the yellow area on Fig. 3(left column) is the largest).

Then, independently of this, one has to chose all other parameters to maximize the factor on the left part of Eqs. (30a-c). For instance, the gap g must be as small as possible, V_{dc} as large as possible… One can also remark that η_{act} does not depend on the device width b, whereas C_{mot} and G_{mot} do: the amount of generated electric charge / current is proportional to b, on the contrary of the beam's elasticity.

Piezoelectric / dielectric actuation In the case of an active layer actuation, one obtains:

$$\eta_{\text{act}} = \frac{3\,e_{31}\, l_b^2}{\xi\, Y_b h_b^2} \underbrace{\frac{D_b}{D_t(1+\kappa)}\left(1+\frac{h_t}{h_b}\right)}_{f_1} \frac{\Phi_i(l_b)[\Phi_{i,x}]_{\bar{x}_-}^{\bar{x}_+}}{\bar{\omega}_i^2} \tag{31a}$$

$$C_{\text{mot}} = \frac{3\,e_{31}^2\, b l_b}{2\xi\, Y_b h_b} \underbrace{\frac{D_b}{D_t(1+\kappa)^2}\left(1+\frac{h_t}{h_b}\right)^2}_{f_2} \frac{\left([\Phi_{i,x}]_{\bar{x}_-}^{\bar{x}_+}\right)^2}{\bar{\omega}_i^2} \tag{31b}$$

$$G_{\text{mot}} = \frac{\sqrt{3}\,e_{31}^2\, b}{4\xi\, l_b\sqrt{\rho_b Y_b}} \underbrace{\frac{1}{(1+\kappa)^2}\sqrt{\frac{m_b D_b}{m_t D_t}}\left(1+\frac{h_t}{h_b}\right)^2}_{f_3} \frac{\left([\Phi_{i,x}]_{\bar{x}_-}^{\bar{x}_+}\right)^2}{\bar{\omega}_i} \tag{31c}$$

where

$$\frac{D_t}{D_b} = 1 + \left(4\frac{h_t^2}{h_b^2} + 6\frac{h_t}{h_b} + 3\right)\frac{h_t Y_t}{h_b Y_b} - \underbrace{3\left(1+\frac{h_t}{h_b}\right)^2 \frac{\kappa}{1+\kappa}}$$

$$\frac{m_t}{m_b} = 1 + \frac{\rho_t h_t}{\rho_b h_b}$$

where here again, the underlined term comes from the axial/bending coupling. The above equations are valid for both piezoelectric and dielectric actuation: for the latter, one has just to use the corresponding value of e_{31} (Eq. (17). Y_t denotes the Young's modulus of the active layer (Y_b or Y_d, depending on the choice of transduction).

We first analyze the effect of the active layer thickness h_t. All terms but $(1+h_t/h_p)$ in Eqs. (31a-c) are decreasing functions of h_t. In particular, the effect of an increase of h_t is to increase

the bending stiffness D_t of the beam, so that the slope difference $[\Phi_{i,x}]_{\bar{x}_-}^{\bar{x}_+}$ of the active layer ends is decreasing.

We now consider the factors f_1, f_2 and f_3 of Eqs. (31a-c), that are functions of h_t/h_b and Y_t/Y_b (and of ρ_t/ρ_b for f_3). They are shown on Fig. 4 as function of h_t/h_b, for several values of Y_t/Y_b. One can observe that for values of Y_t/Y_b higher than $\simeq 0.3$, the f_i are decreasing functions of h_t/h_b. For common piezoelectric / dielectric materials, their Young modulus is higher than the one of the beam material (silicon, steel, aluminium...), so that the ratio Y_t/Y_b is higher than one or at least close to. As a consequence, since all terms decrease faster than $(1 + h_t/h_p)$ increases as a function of h_t, *the optimal thickness of the active layer is zero !*

This paradoxical effect can be explained by considering the mechanical effect of the active layer. When actuated by a voltage $\tilde{V}$, it tends to change its length, which creates an axial force on the beam that is applied at a distance $d = (h_t + h_b)/2$ from the neutral axis. This force is $be_{31}\tilde{V}$ (obtained by integrating Eq. (5a) over the active layer cross-section): *it does not depend on* h_t. As conclusion, increasing h_t increases the distance d and consequently the equivalent bending moment, but this has a lesser effect than the increase of bending stiffness of the beam. As seen above, this effect is opposite if Y_t/Y_b is small.

In practice, h_t has to be chosen so that the electric field $E_z = \tilde{V}/h_t$ in the active layer is smaller than its breakdown value, above which the active layer becomes conductive.

Since h_t has to be chosen as small as possible, the mechanical effect of the active layer on the elasticity of the beam can be neglected in a first approach. The slope difference $[\Phi_{i,x}]_{\bar{x}_-}^{\bar{x}_+}$ has thus to be chosen as large as possible, by considering a particular mode shape of a standard cantilever beam. Fig. 3(right column) illustrates the best location and length of the dielectric layer. Again, i solutions are possible for mode i, with the best one being associated to an active layer located at the free end of the beam (shown in yellow on Fig. 3(right column)).

Since in practice the active layer has a non zero thickness, a fine optimization of x_- and l_t can be done for modes higher than the first one, by maximizing $[\Phi_{i,x}]_{\bar{x}_-}^{\bar{x}_+}$ with a mechanical model that includes the increase of mass and stiffness due to the active layer.

Finally, if a dielectric layer is considered, its thickness h_t also appears in e_{31}, which add another decreasing term as a function of h_t. The above results (one has to choose h_t as small as possible) are thus even more valid for a dielectric layer.

Optimization with the coupling factor criterion

The situation is by far different if the MEMCF is used as optimization criterion. It has been shown in [7] that a non zero optimal thickness is found in any cases, which leads to optimal length and location of the active layer. This is due to the fact that following Eq. (27), k_i is inversely proportional to the electric capacitance C of the piezoelectric layer, in addition to its dependence on χ_i and K_i. All those quantities depend on the thickness h_t and the length l_t of the active layer and those effects can cancel each other. As a consequence (see [7, 8]), since the optimal thickness h_t can be large as compared to the one of the beam, *the mechanical influence of the active layer must be taken into account in the optimization computation*. This leads to the optimal geometries shown on Fig. 5, where it is clear that the mechanical effect of the active layer influences the deformed shape of the beam. This figure can be compared to Fig. 3 to see the optimization differences. For further details, see [7], especially for quantitative values of the optimal length, thickness and location of the active layers.

For the two other transduction principles, analogous results may be obtained. However, since vibration damping with passive shunt applications are a priori reserved to macro-structures, this optimization is not considered here for a sake of brevity.

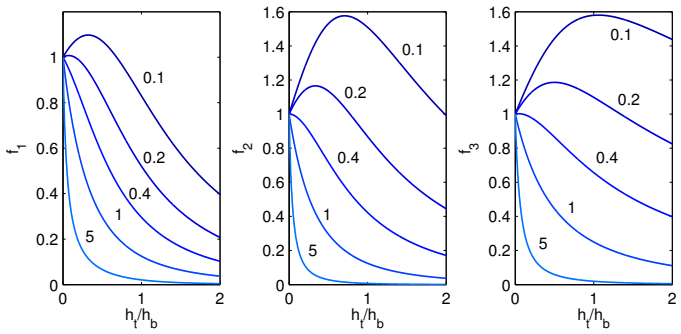

Figure 4. FACTORS f_1, f_2 AND f_3 AS A FUNCTION OF h_t/h_b. THE VALUES OF Y_t/Y_b ARE INDICATED ON THE FIGURE AND $\rho_t/\rho_b = 1$.

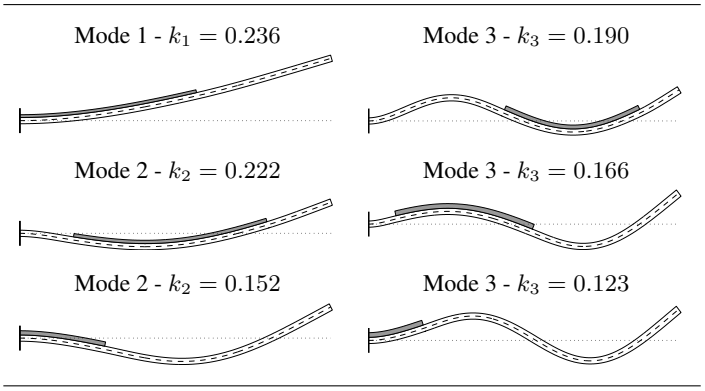

Figure 5. DEFORMED SHAPES OF THE OPTIMAL CONFIGURATIONS FOR AN ALUMINIUM / PIC151 BEAM CONSIDERING THE COUPLING FACTOR CRITERION (FROM [7]).

CONCLUSION

In this paper, three transduction principles have been compared (electrostatic, piezoelectric and dielectric), in term of their efficiency and of the optimization of the geometry of the active part of the devices.

The first result is that the transduction principle of a dielectric layer *is electromechanically equivalent* to that of a piezoelectric layer. A similar constitutive law can be written, with a modified e_{31} (or d_{31}) coefficient, so that any model used to design a piezoelectric structure can be equally used for dielectric layers.

The second result is that the dielectric layer transduction principle is theoretically as efficient as the piezoelectric and electrostatic ones, provided thin films of dielectric material with a high permittivity are used. The thickness of the active layer must be of the order of several tenth of nanometers, so that this transduction principle is adapted only for nanostructures (the same conclusion holds for the electrostatic transduction).

Finally, several optimization criteria have been considered. It has been shown that if the device is used as a resonator, for which one is interested in maximizing the resonance motion, the thickness of the active layer has to be as thin as possible, so that a model that neglects the mechanical effect of the active layers is sufficient for the optimization. On the contrary, using the electromechanical coupling factor as an optimization parameter leads to an optimal thickness of the active layer that can be of the same order of magnitude than the one of the beam, so that a proper model must include the mechanical effect of the active layer.

REFERENCES

[1] Preumont, A., 2011. *Vibration Control of Active Structures*. Springer.

[2] Anton, S. R., and Sodano, H. A., 2007. "A review of power harvesting using piezoelectric materials (2003-2006)". *Smart Materials and Structures,* **16**, pp. R1–R21.

[3] Younis, M. I., 2011. *MEMS Linear and Nonlinear Statics and Dynamics*. Springer.

[4] Dezest, D., Thomas, O., Mathieu, F., Mazenq, L., Soyer, C., Costecalde, J., Remiens, D., Deü, J.-F., and Nicu, L., 2015. "Wafer-scale fabrication of self-actuated piezoelectric nanoelectromechanical resonators based on lead zirconate titanate (pzt)". *Journal of Micromechanics and Microengineering,* **25**(3), p. 035002. doi:10.1088/0960-1317/25/3/035002.

[5] Karabalin, R. B., Matheny, M. H., Feng, X. L., Defaÿ, E., Rhun, G. L., Marcoux, C., Hentz, S., Andreucci, P., and Roukes, M. L., 2009. "Piezoelectric nanoelectromechanical resonators based on aluminum nitride thin films". *Applied Physics Letters,* **95**, p. 103111.

[6] Bouwstra, S., Blom, F. R., Lammerink, T. S. J., Yntema, H., Schrap, P., Fluitman, J. H. J., and Elwenspoek, M., 1989. "Excitation and detection of vibrations of micromechanical structures using dielectric thin film". *Sensors & Actuators,* **17**, pp. 219–223.

[7] Ducarne, J., Thomas, O., and Deü, J.-F., 2012. "Placement and dimension optimization of shunted piezoelectric patches for vibration reduction". *Journal of Sound and Vibration,* **331**(14), pp. 3286–3303.

[8] Sénéchal, A., Thomas, O., and Deü, J.-F., 2010. "Optimization of shunted piezoelectric patches for vibration reduction of complex structures - application to a turbojet fan blade". In Proceedings of the ASME IDETC/CIE 2010 conference.

[9] Thomas, O., Deü, J.-F., and Ducarne, J., 2009. "Vibration of an elastic structure with shunted piezoelectric patches: efficient finite-element formulation and electromechanical coupling coefficients". *International Journal of Numerical Methods in Engineering,* **80**(2), pp. 235–268.

[10] Pelesko, J. A., and Bernstein, D. H., 2003. *Modeling MEMS and NEMS*. Chapman & Hall / CRC.

[11] Tiersten, H. F., 1969. *Linear piezoelectric plate vibrations*. Plenum Press.

[12] Griffiths, D. J., 1999. *Introduction to electrodynamics*, 3rd. ed. Prentice Hall.

[13] Thomas, O., Ducarne, J., and Deü, J.-F., 2012. "Performance of piezoelectric shunts for vibration reduction". *Smart Materials and Structures,* **21**(1), p. 015008.

[14] Berardengo, M., Manzoni, S., Thomas, O., and Giraud-Audine, C., 2015. "A new electrical circuit with negative capacitance to enhance resistive shunt damping". In Proceedings of SMASIS 2015 (ASME 2015 Conference on Smart Materials Adaptive Structures and Intelligent Systems), p. 8836.

[15] Ducarne, J., Thomas, O., and Deü, J.-F., 2010. "Structural vibration reduction by switch shunting of piezoelectric elements: modelling and optimization". *Journal of Intelligent Materials Systems and Structures,* **21**(8), pp. 797–816.

[16] Lesieutre, G. A., and Davis, C. L., 1997. "Can a coupling coefficient of a piezoelectric device be higher than those of its active material?". *Journal of Intelligent Material Systems and Structures,* **8**(10), pp. 859–867.